Two-step mechanism of spiral phyllotaxis

Two-step mechanism of spiral phyllotaxis

Short title: Two-step mechanism of phyllotaxis

Authors: Takuya Okabe[1] and Jin Yoshimura[2,3,4,5,6]

Affiliations:

[1]Graduate School of Integrated Science and Technology, Shizuoka University, 3-5-1 Johoku, Hamamatsu 432-8561, Japan

[2]Department of International Health and Medical Anthropology, Institute of Tropical Medicine, Nagasaki University, Nagasaki 852-8523, Japan

[3]Department of Biological Sciences, Tokyo Metropolitan University, Hachioji, Tokyo, 192-0397 Japan

[4]The University Museum, University of Tokyo, Bunkyo-ku, Tokyo, 113-0033 Japan

[5]Marine Biosystems Research Center, Chiba University, Uchiura, Kamogawa, Chiba 299-5502, Japan

[6]Department of Environmental and Forest Biology, State University of New York College of Environmental Science and Forestry, Syracuse, NY 13210, USA

Corresponding author: Takuya Okabe (okabe.takuya@shizuoka.ac.jp)

Keywords: canalization, parallel evolution, convergent evolution, plant morphology, epigenetics

Abstract:

Fibonacci numbers such as 5, 8, and 13 occur in the spiral arrangement of lateral organs at shoot tips in plants. While the cone scales of conifers are normally arranged in 5 and 8 (or 8 and 13) curved rows in opposite directions, other numbers such as 4 and 7 (or 7 and 11) are found anomalously. The observed numbers still obey the Fibonacci rule, with the next number being the sum of the preceding two. Although these observations have been made for centuries, the underlying mechanisms of the numerical relationship have not been investigated. Here, we show that this phenomenon is caused by a two-step mechanism: (1) maintenance of a constant angle between consecutive lateral organs and (2) strong canalization of this angle to a specific value. The first step of the mechanism precedes the second step of the mechanism because the Fibonacci-rule pattern is due to the first step, while the second step distinguishes normal, anomalous and unobserved types. The current dominance of the normal type is a result of the evolutionary process of the second step.

INTRODUCTION

Phyllotaxis is the arrangement of leaves, scales and flower parts around the plant stem. The most common mode of arrangement is spiral phyllotaxis, in which Fibonacci numbers occur everywhere. The Fibonacci numbers 1, 2, 3, 5, 8, 13, … obey the Fibonacci-rule pattern in which every number is the sum of the two preceding numbers. On a pinecone, curved rows of scales (parastichies) run in two opposite directions, one clockwise and the other counterclockwise. Typically, 5 shallow curves and 8 steep curves are observed, while 13 steeper curves may be more visible than 5 curves if the cone is observed from below (Fig. 1(a)). There are as many left-handed cones as right-handed cones if handedness is defined by the most conspicuous spirals. While patterns with Fibonacci numbers such as 5:8 are overwhelmingly more common, anomalous types with similar numbers such as 4:7 and 6:10 are occasionally found. The Fibonacci-rule pattern in the normal type holds for the numbers in any anomalous type (Braun 1831). The difference between normal and anomalous types lies in the two seed numbers that begin the Fibonacci-rule pattern. Fibonacci numbers (normal type) begin with 1 and 2, followed by 3, 5, 8 and so on. Therefore, the normal type is denoted as type $\langle 1,2 \rangle$. The number pair 4:7 of an anomalous pattern is a member of type $\langle 1,3 \rangle$ because it belongs to a Fibonacci-like sequence including 1, 3, 4, 7, 11, etc. (often called Lucas numbers). Similarly, a 6:10 pattern is an anomaly of type $2\langle 1,2 \rangle$, as the first numbers (2 and 4) of the sequence 2, 4, 6, 10, 16, ... are twice those (1 and 2) of the normal type.

Existing empirical studies on anomalous types are only descriptive (Jean 1994). In fact, the adaptive significance of the phyllotaxis phenomenon is far from obvious. Normal

and anomalous patterns look so similar that they are difficult to tell apart at a glance. Indeed, some studies have attempted to establish an ultimate causal relationship between phyllotaxis and light capture efficiency, although with inconclusive results (Niklas 1988, Valladares and Brites 2004). Even if adaptation to the environment is irrelevant for phyllotaxis, few biologists today would question the importance of investigating the ultimate as well as proximate causalities of biological phenomena (Mayr 1988; Okabe et al. 2019). Recent investigations have shown that phyllotaxis is an internal adaptation for which normal and anomalous types are optimal and suboptimal solutions to the same optimization problem (Okabe 2015; Okabe and Yoshimura 2016). Owing to the obscurity of anomalies, unfortunately, no comparative study has been conducted with different types, either physiologically or ecologically. Here, we investigate a mathematical lattice pattern of q and q' spirals crossing with each other, where the two numbers q and q' are arbitrary numbers, i.e., not necessarily Fibonacci numbers. The lattice model provides a theoretical framework for describing general patterns including not only existing spiral and non-spiral patterns but also the patterns that do not exist in nature. The model description is instructive to underline the significance of the problem that the existing patterns appear to have nothing special as compared with non-existing patterns. Why only some special patterns are observed, but not others? To elucidate the differences among normal, anomalous and unobserved patterns, theoretically possible number pairs (q:q') are plotted on a two-dimensional graph, which suggests two independent rules: one for the Fibonacci-rule pattern and the other for distinguishing between various types. Based on these rules, general predictions may be made about the abundance of anomalies in any species,

including those yet to be investigated. Furthermore, these rules, if correct, may provide the groundwork for establishing underlying developmental mechanisms of the phyllotaxis phenomena. We would like to stimulate new studies on the genetics, physiology, ecology and evolution of this centuries-known phenomenon.

Before moving to the main subject of this study, it should be remarked that this paper does not discuss physiological details of the developmental mechanism of pattern formation. Recent theoretical studies on leaf primordia generation have successfully reproduced various phyllotaxis patterns observed in higher plants (Douady and Couder 1996abc; Fujita and Kawaguchi 2018; Yonekura et al. 2019). In these models, developmental constraints on leaf primordia formed at the periphery of the apical meristem are emphasized as the reason why some specific patterns are observed preferentially. No doubt this is an important explanation at the developmental level. However, it is not the ultimate explanation in view of the fact that, just like a model of a dynamical system in physics, dynamical models of developmental mechanisms are discussed with little or no attention to the evolutionary history of plants, i.e., to the ultimate question of why the developmental constraints are brought about. This is a problem on the adaptive value or the meaning of the observed patterns. In this respect, we stress the importance of investigating the significance of observed patterns as compared with those not observed, because there is no doubt that patterns and the formation mechanism have been evolved by natural selection. While rare patterns may be considered as a result of a developmental error (anomaly), they are variants of polymorphism requiring a phylogenetic and ecological explanation. Two steps of mechanism put forward in the present study may not be

distinguished in the dynamical-model explanation, but they can be from an evolutionary and ecological perspective. As a pattern analysis of theoretical nature, we do not delve into specific details of pattern formation mechanism.

MODEL AND RESULTS

We investigate a lattice on a cylindrical surface (stem of a shoot) consisting of q spirals in one direction and q' spirals in the other direction. Formally, a q:q' phyllotaxis pattern is obtained by rolling a grid paper such that two points separated by q and q' units in the x and y directions, respectively, are on top of each other (Fig. 1(b,c)). A plane view of the q:q' system is obtained by cutting the cylindrical surface along a vertical line and spreading it back on a plane (Fig. 1(d)). Plants make this pattern by producing leaves (grid points) successively in the order of their height. To indicate birth order, the points are numbered from below (Fig. 1(e)). The angular interval and the height distance between two consecutive leaves are called the divergence angle and rise, respectively (Fig. 1(e)). q:q' number pairs are classified according to their greatest common divisor J, as it represents the number of leaves (points) at each height (rise). Only if q and q' have no common divisor except 1, such as q:q'=2:3 (J=1), a single leaf occurs at each height (Fig. 1(d,e)). If the greatest common divisor J is not 1, such as q:q'=4:6 (J=2), then J leaves occur at each height (rise; technically, this is height distance measured relative to the circumference length). Thus, a 4:6 pattern has 2 opposite leaves at each rise, and this pattern is formally a 2:3 pattern repeated twice around the axis (Fig. 1(f)). The angular interval (divergence angle) and the height distance (rise) between two consecutive leaves are measured relative

to the circumference of the stem cylinder (Fig. 1(e)). Therefore, the divergence angle and the rise of a 4:6 pattern are half the corresponding values for a 2:3 pattern. Each *q*:*q'* pattern has unique values of divergence angle and rise. In plotting *q*:*q'* number pairs on a two-dimensional graph, it is convenient to use the square root of rise/*J* as the *y*-axis because it represents the organ size ratio *D/C*, i.e., the ratio of the diameter *D* of the organ (vertical circle in Fig. 1(g)) to the cylinder circumference *C* (horizontal circle in Fig. 1(g)). If the lattice pattern is transformed to logarithmic spirals on a shoot tip (bud), the ratio *D/C* is the size ratio of a primordium to the shoot apex (Fig. 1(h)) (Supplementary Information) (Schwendener 1878; Church 1904; Richards 1951). Thus, the *q*:*q'* number pairs are plotted against the divergence angle and *D/C* (Fig. 2(a,b)). These results demonstrate two points: (i) the empirical rule of the Fibonacci-rule pattern for *q:q'* indicates that the divergence angle is fixed, and (ii) each sequence has its own value at which the angle is fixed. The natural dominance of a normal sequence (1, 2, 3, 5, 8, …) indicates that the angle is strongly canalized to a specific value (137.5°). The point size in Fig. 2 represents the order (in frequency of natural occurrence) of each *q*:*q*' pair (see below). The largest points on the solid lines (Fig. 2(a,b)) are the normal type ⟨1,2⟩. The smallest points either do not exist or are inconclusive. Major and minor anomalous types (⟨1,3⟩, 2⟨1,2⟩ and ⟨2,5⟩, ⟨1,4⟩) are plotted with intermediate-sized points on dashed and dotted lines, respectively. Type ⟨1,2⟩ has a constant divergence angle of 137.5°. Anomalous types ⟨1,3⟩ and 2⟨1,2⟩ have a constant divergence angle of 99.5° (dashed line in Fig. 2(a)) and 69° (dashed line in Fig. 2(b)), respectively.

DISCUSSION

In seed plants, the organ size ratio *D/C* decreases as the shoot grows from the seedling stage to the flowering stage. Accordingly, the number pair *q*:*q'* may vary during growth in accordance with the Fibonacci-rule pattern (Fig. 2(c-e)). The increase/decrease in *q*:*q'* due to variation in *D/C* is called rising/falling phyllotaxis (Jean 1994). For the florets on a sunflower head, the number pair *q*:*q'* of curved spirals (parastichies) decreases from the rim towards the center, e.g., from 34:55 through 21:34, 13:21, and 8:13 to 5:8. This decrease is due to an increase in *D/C* as the apex size *C* shrinks while being filled with floral primordia. In this empirical observation, the obeyance of the Fibonacci rule and the predominance in nature of Fibonacci numbers (1, 2, 3, 5, 8, …) are two distinct issues. Not all theoretically possible Fibonacci-related sequences are observed in nature; instead, only limited sequences occur with extremely biased frequencies. There are channels of allowed values of the divergence angle to which a sporadic failure of canalization may lead.

For reference, Table 1 shows the frequency of occurrences of various types of cones from a single tree of European black pine (*Pinus nigra*) (Fierz 2015). In a total of 6000 cones, 97% exhibit the normal pattern 8:13 of type $\langle 1,2 \rangle$. Accordingly, a randomly selected cone is almost certain to be a normal cone. The remaining 3% include nine anomalous types. In the last column of the table, we added the mean probability and standard deviation $p \pm \sigma$ by assuming a binomial distribution; $p = M/N$ is the number M of cones divided by the total number $N = 6000$ and $\sigma = \sqrt{p(1-p)/N}$. Data with $p - 2\sigma > 0$ are shown in

bold to indicate statistical significance. The most frequent anomalous pattern was 10:16 (type 2⟨1,2⟩), with a frequency of approximately 1%, and the second most frequent pattern was 7:11 (type ⟨1,3⟩). These results are a general empirical rule (see below). In any species, anomalies are mostly of types 2⟨1,2⟩ and ⟨1,3⟩, while the rest of the samples contain a few minor types including ⟨2,5⟩, ⟨1,4⟩ and 3⟨1,2⟩. The observed types ⟨1,2⟩, 2⟨1,2⟩, ⟨1,3⟩, ⟨2,5⟩, ⟨1,4⟩ and 3⟨1,2⟩ are characterized by divergence angles of 137.5°, 69°, 99.5°, 151°, 78° and 46°, respectively. These angles have been directly observed on the shoot tip of a handful of investigated species, i.e., *Opuntia kuntzei* (*Pterocactus kuntzei*; 137.5°, 78°, and 69°) (Bilhuber 1933), *Araucaria columnaris* (*Araucaria excelsa*; 46°) (Barthelmess 1935), *Cunninghamia lanceolata* (99.5°) (Fujita 1939), and *Cephalotaxus harringtonii* (*Cephalotaxus drupacea*; 137.5°, 69°, and 151°) (Fujita 1937,1939; Camefort 1956). If these anomalous patterns are regarded as developmental anomalies, they must be distinguished from irregular patterns. Anomalous patterns are as regular as a normal pattern. As is typical of biological phenomena, irregular anomalies are not rare. The irregular patterns in Table 1 are not classifiable because they do not have a consistent parastichial pattern, owing to accidental loss or addition of a parastichial spiral due to growth irregularities (Bravais and Bravais 1837; Fierz 2015).

The nontriviality of the predominance of normal type ⟨1,2⟩ cannot be overemphasized. Accurate control of divergence angle is evidenced by the striking contrast between the observed number (5838) of instances of 8:13 (137.5°) and the total absence of instances of 8:11 (133.2°) (Table 1, Fig. 2(a)). Theoretically, these two patterns are indistinguishable at a glance (Fig. 2(e,f)). A sporadic failure of canalization to the normal

8:13 pattern (⟨1,2⟩, 137.5°) leads directly to either 10:16 (2⟨1,2⟩, 69°) or 7:11 (⟨1,3⟩, 99.5°) but is extremely unlikely to produce similar patterns such as 8:11 (⟨3,8⟩, 132°), 7:10 (⟨3,7⟩, 106°), 10:14 (2⟨2,5⟩, 75°), and 10:15 (5⟨1,2⟩, 46°). Similar patterns have similar values of the organ size ratio *D/C*. Thus, the observation suggests not only that canalization to normal and anomalous types has a common underlying mechanism but also that the channel is sporadically switched among certain definite types that are predetermined independently of *D/C*.

Table 2 is based on conifer cones of various species (Brousseau 1969). The number of anomalous types was recorded for individual trees, while no distinction was made among them. For the lodgepole pine (*P. murrayana*), four of eight anomalies came from a single tree. Similarly, a single tree produced 13 of 18 anomalies for the Jeffrey pine (*P. jeffreyi*) and 5 of 7 for the Monterey pine (*P. radiata*). No details were provided for the high frequency (8%) in *P. balfouriana* (foxtail pine). Thus, these data suggest another general rule: the occurrence rates of anomalies depend not only on species but also on individuals. Consistent with the abovementioned result, on average, anomalous types comprise approximately one or two percent of the population, depending on whether the foxtail pine is excluded. Consequently, we expect that the occurrence of anomalous types depends on ecology and geography, reflecting the evolution and dispersion of the plant. A comprehensive ecological survey is needed to draw a definite conclusion on the frequency and distribution of anomalies. To summarize, we may draw the following conclusions from our observations. (i) Any species with spiral phyllotaxis (typically type ⟨1,2⟩) has anomalous (atypical but not irregular) types. (ii) The total frequency of anomalous types is

on the order of 1%, while the exact value depends on species. (iii) Individuals produce a significantly high rate of anomalies. (iv) The majority of anomalous patterns are of types $2\langle 1,2\rangle$ and $\langle 1,3\rangle$, while the rest are of a few minor types such as $3\langle 1,2\rangle$, $\langle 2,5\rangle$ and $\langle 1,4\rangle$. The other types are extremely rare (<0.1%) or nonexistent.

The underlying mechanism of canalization to the optimal angle is unknown. Although the available data are mostly for conifer cones, the conifers are of interest only as the most typical example in which the golden angle (137.5°) controlling the growth and pattern formation of every leafy shoot is visible to the naked eye. Phyllotaxis is a very general phenomenon, including both spiral and non-spiral arrangements (Okabe et al. 2019). New developmental and ecological comparative studies may be carried out in any convenient systems if only researchers' attention is directed to the elusive difference in phyllotaxis type. There is no essential difference among the patterns of a pinecone, a rosette, and a transverse section of a shoot tip (Fig. 3). Divergence angle may be directly observed in a top view of a cone, while it should be noted that arrangement near the cone tip can be secondarily deformed (Fig. 3(d-f)). A pentagon may be visible for normal type $\langle 1,2\rangle$ (Fig. 3(d)). In an anomalous 6:10 pattern of type $2\langle 1,2\rangle$, two opposite scales are successively rotated by 69°. In Fig. 3(e), a supplementary angle (180-69=111°) is used to highlight a hexagon of double triangles. A skewed square may be seen in an anomalous 4:7 pattern of type $\langle 1,3\rangle$, as the angle (99.5°) is almost a right angle (Fig. 3(f)). In all cases, characteristic polygons are rotated gradually as leaves (scales) are followed in their initiation order. In mature patterns of elongated shoots, leaves connected by vascular strands are straightened vertically. Consequently, the polygonal shape is made so obvious that the fractional

representation of the divergence angle, such as 1/3 or 2/5 of type $\langle 1,2 \rangle$ and 1/4 or 2/7 of $\langle 1,3 \rangle$, becomes valid (Braun 1831; Van Iterson 1907; Snow and Snow 1934; Esau 1965).

To randomly select a one-percent anomaly is like a game of chance. In each trial, an anomaly is drawn with a probability of one in a hundred ($H = 100$). How many trials are needed to find an anomaly? In H trials, the chance of no anomaly is still high (38%) because the probabilities of drawing zero, one, and more than one anomaly are approximately the same. In terms of the probability $p = 1/H$ of a single trial, the probability of drawing none in a total of c times H trials is given by $1/\mathrm{e}^c$ for $H \gg 1$, which is 0.14 for c=2 and 0.05 for c=3. The factor $p - 2\sigma$ becomes positive if at least five anomalies are drawn. For $p = 1/100$, the chance of drawing one anomaly is high in 200 trials (86%) and almost certain in 300 trials (95%); 500 trials would make the results statistically reliable. According to this estimation, approximately 300 cones in two species of Japanese conifer, on which no report has been made, were examined. One instance of 4:6 (type $2\langle 1,2 \rangle$) in *P. densiflora* and two instances each of 6:10 (type $2\langle 1,2 \rangle$) and 7:11 (type $\langle 1,3 \rangle$) in *P. thunbergii* were found at three locations (Fig. 3(e,f)). Thus, anomalous types very likely remain undiscovered in economically important families that have been intensively studied, including the crucifers (Brassicaceae), the cucurbits (Cucurbitaceae), the legumes (Fabaceae), and the nightshades (Solanaceae). Indeed, there is a brief mention of an anomalous 4:7 leaf pattern in a branded daikon radish (*Raphanus sativus*) (Koriba 1951) (Fig. 3(h)). The species dependence of the frequencies of anomalous types should reflect the strength of selection pressure for phyllotaxis mechanisms. It appears unlikely that herbaceous plants that do not exhibit conspicuous regularity have been under selection

pressure as strong as that on conifer trees. The abovementioned assumption ($H = 100$) on the relative abundance of the normal type can generally be considered an overestimate. Anomalous phyllotaxis types might be unexpectedly common.

The present study provides a new direction for investigating spiral phyllotaxis mechanisms. The model analyses indicate suspected canalization of the divergence angle towards the golden angle 137.5°, which we claim is the key factor for the occurrence of Fibonacci numbers in phyllotaxis. In anomalous phyllotaxis, the divergence angle is canalized into one of the predetermined values. Owing to this canalization, the Fibonacci-rule pattern always holds, irrespective of whether the phyllotaxis is normal. We predict the existence of Fibonacci-type spiral phyllotaxis anomalies of approximately one percent for any plant species, which should be tested by future ecological studies. Moreover, experimental studies should demonstrate the heritability and homeostasis of the predicted canalization. The comparative molecular approach could be used by comparing the genetic backgrounds of both normal and anomalous phyllotaxis patterns. The common rules of phyllotaxis are observed in various lineages from seed plants, ferns, mosses to brown algae, implying parallel/convergent evolution (Braun 1831; Church 1904; Yoshida 1983; Okabe et al. 2019). Empirical observations (Bravais and Bravais 1837; Brousseau 1969; Jean 1994; Fierz 2015) strongly suggests epigenetic control of suspected canalization. Therefore, the presented view provides the first insight into the underlying mechanisms of spiral phyllotaxis.

References

Barthelmess A (1935) Über den Zusammenhang zwischen Blattstellung und Stelenbau unter besonderer Berücksichtigung der Koniferen. Botanisches Archiv 37: 207–260.

Bilhuber E (1933) Beiträge zur Kenntnis der Organstellungen im Pflanzenreich. Botanisches Archiv. 35:188-250.

Braun A (1831) Vergleichende Untersuchung über die Ordnung der Schuppen an den Tannenzapfen als Einleitung zur Untersuchung der Blattstellung. Nov. Acta Ac. CLC 15: 195–402.

Bravais L, Bravais A (1837) Essai sur la disposition des feuilles curvisériées. Annales des Sciences Naturelles Botanique 7: 42–110.

Brousseau A (1969) Fibonacci statistics in conifers. Fib. Q. 7: 525-532.

Camefort H (1956) Étude de la structure du point végétatif et des variations phyllotaxiques chez quelques Gymnospermes. Ann. Sci. Nat. Bot. Biol. Veg. XI 17: 1–185.

Church AH (1904) On the Relation of Phyllotaxis to Mechanical Laws, Williams & Norgate, London.

Douady S, Couder Y (1996a) Phyllotaxis as a Dynamical Self Organizing Process Part I: The Spiral Modes Resulting from Time-Periodic Iterations. J. Theor. Biol. 178, 255-274.

Douady S, Couder Y (1996b) Phyllotaxis as a Dynamical Self Organizing Process Part II: The Spontaneous Formation of a Periodicity and the Coexistence of Spiral and Whorled Patterns. J. Theor. Biol. 178, 275-294.

Douady S, Couder Y (1996c) Phyllotaxis as a Dynamical Self Organizing Process Part III:

The Simulation of the Transient Regimes of Ontogeny. J. Theor. Biol. 178, 295-312.

Esau E (1965) Vascular differentiation in plants, Holt, Rinehart and Winston, New York.

Fierz V (2015) Aberrant phyllotactic patterns in cones of some conifers: a quantitative study. Acta Soc. Bot. Pol. 84: 261-265.

Fujita H, Kawaguchi M. Spatial regularity control of phyllotaxis pattern generated by the mutual interaction between auxin and PIN1. PLOS Comp Biol. 2018; 14: e1006065.

Fujita T (1937) Über die Reihe 2,5,7,12 …. in der schraubigen Blattstellung und die mathematische Betrachtung verschiedener Zahlenreihensysteme. Bot. Mag. Tokyo 51: 480–489.

Fujita T (1939) Statistische Untersuchungern über den Divergenzwinkel bei den schraubigen Organstellungen. Bot. Mag. Tokyo 53:194–199.

Jean RV (1994) Phyllotaxis: a systemic study in plant morphogenesis, Cambridge University Press, Cambridge.

Koriba K (1951) Shokubutsu no Kikankeisei, Iwanami Shoten, Tokyo.

Mayr E (1988) Toward a New Philosophy of Biology: Observations of an Evolutionist, Harvard University Press, Cambridge.

Niklas KJ (1988) The Role of Phyllotactic Pattern as a “Developmental Constraint” On the Interception of Light by Leaf Surfaces. Evolution 42:1-16.

Okabe T et al (2019) The unified rule of phyllotaxis explaining both spiral and non-spiral arrangements. J. Royal Soc. Interface 16: 20180850.

Okabe T (2015) Biophysical optimality of the golden angle in phyllotaxis. Sci. Rep. 5: 15358.

Okabe T, Yoshimura J (2016) Optimal hash arrangement of tentacles in jellyfish. Sci. Rep. 6: 27347.

Richards FJ (1951) Phyllotaxis: Its quantitative expression and relation to growth in the apex. Phil. Trans. Roy. Soc. London 235B: 509-564.

Schwendener S (1878) Mechanische Theorie der Blattstellungen, Engelmann, Leipzig.

Snow M, Snow R (1934) The interpretation of phyllotaxis, Biol. Rev. 9:132-137.

Valladares F, Brites D (2004) Leaf phyllotaxis: Does it really affect light capture? Plant Ecology 174: 11–17.

Van Iterson G (1907) Mathematische und Mikroskopisch-Anatomische Studien über Blattstellungen, Gustav Fischer, Jena.

Yonekura T, Iwamoto A, Fujita H, Sugiyama M. (2019) Mathematical model studies of the comprehensive generation of major and minor phyllotactic patterns in plants with a predominant focus on orixate phyllotaxis. PLoS Comput. Biol. 15(6), e1007044.

Yoshida T (1983) Japanese species of Sargassum subgenus Bactrophycus (Phaeophyta, Fucales). Journal of the Faculty of Science, Hokkaido University. Series 5, Botany 13: 99-246.

Acknowledgments

This work was partly supported by grants-in-aid from the Japan Society for the Promotion of Science (nos. 22255004, 22370010, 26257405, and 15H04420 to JY).

Author contributions: TO conceived and performed the study. TO and JY wrote the manuscript.

Competing financial interests: The authors declare no competing financial interests.

Data availability: No datasets were analyzed during the current study.

Figures

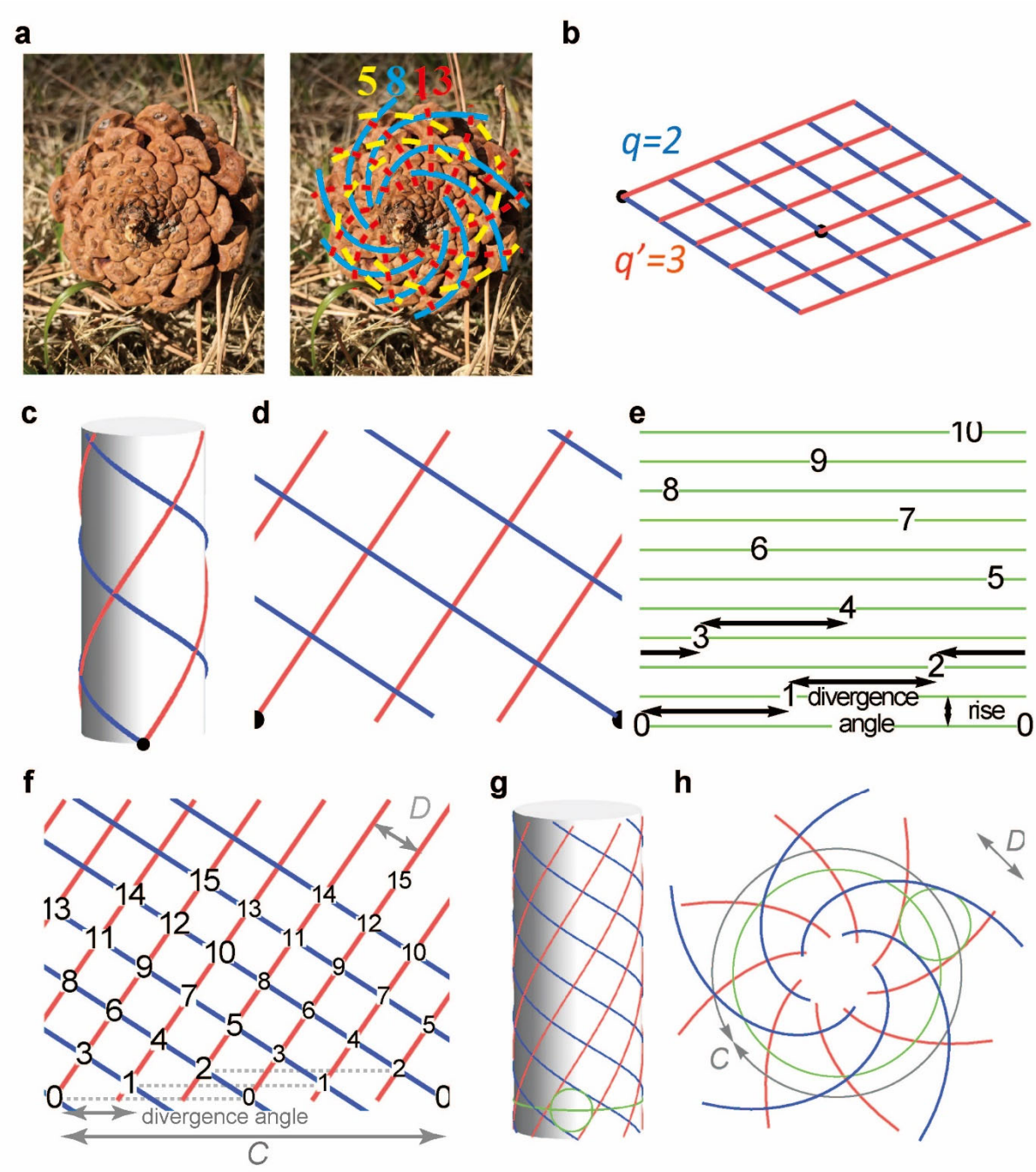
a
5 8 13
b
q=2
q'=3
c
d
e
10
9
8
7
6
5
4
3
2
1
0
divergence angle
rise
0
f
D
15
14
13
12
11
10
9
8
7
6
5
4
3
2
1
0
divergence angle
C
g
h
D
C

Figure 1: Opposed parastichial pair *q*:*q'*. **(a)** A conifer cone showing 5, 8 and 13 spirals (parastichies) as indicated with dashed, solid and dotted lines, respectively (*Pinus thunbergii*). Since the 8 parastichies run in the opposite direction to the 5 and 13 parastichies, this cone has an opposed parastichial pair of 5:8 or 8:13, depending on the point of observation. **(b)** Two points separated by *q*:*q'*=2:3 are marked on a grid paper. **(c)** A *q:q'* pattern is obtained on a cylindrical surface by rolling the paper to match the two points. **(d)** A plane view of the *q:q'* pattern is obtained by cutting the cylinder vertically through the matched points. **(e)** Divergence angle and rise are defined as the horizontal and vertical spacing between consecutive grids numbered from below. **(f)** A 4:6 pattern is a 2:3 pattern repeated twice. The former thus consists of a succession of two leaves at each rise (connected by a gray dotted line). Parameters *C* and *D* are defined as the circumference and mesh size, respectively. **(g)** The parameter *D* is the diameter of an inscribed circle, while the parameter *C* is the girth of the cylinder. **(h)** Logarithmic spirals on a plane, corresponding to the *q*:*q'* pattern in g. In the transformed pattern, the parameters *C* and *D* represent apex size and primordium size, respectively. gh; *D/C*=0.106 for *q*:*q'*=5:8.

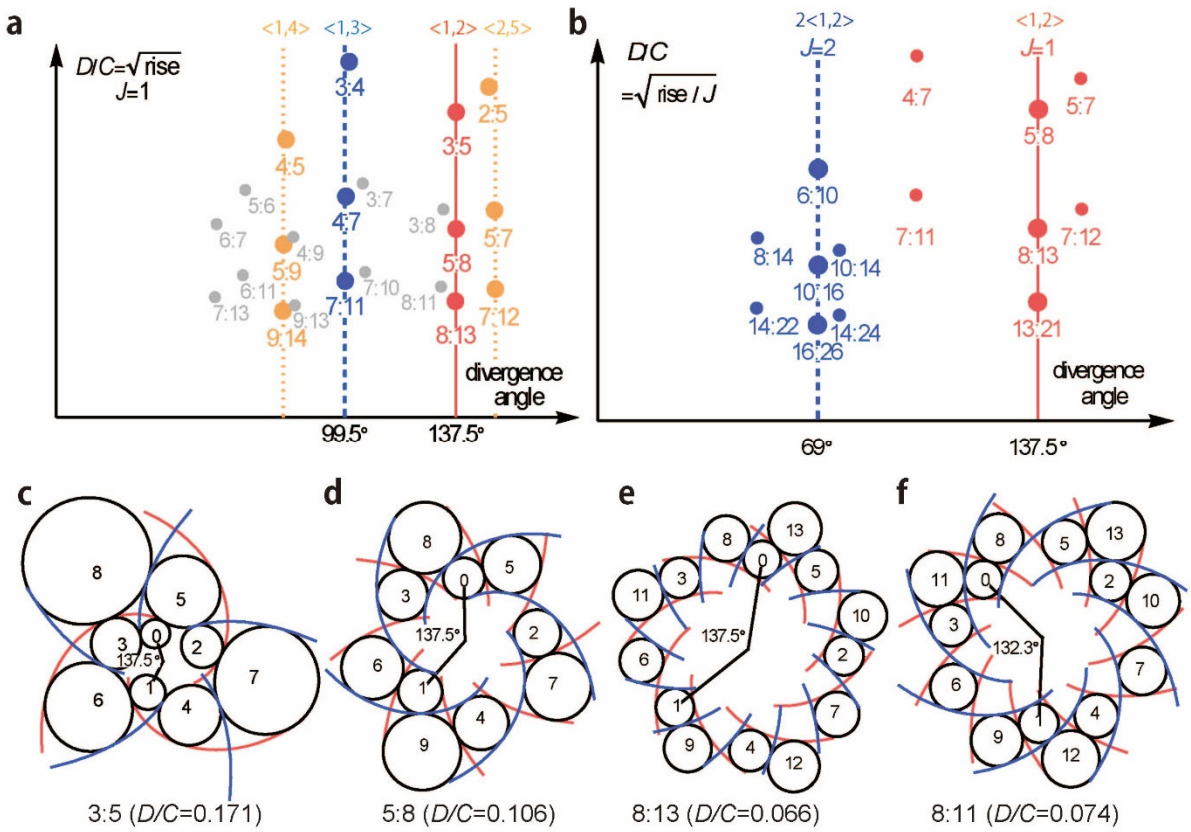

Figure 2. Divergence angle and *D/C* of possible *q:q'* pairs. **(a)** *q:q'* pairs with the greatest common divisor *J*=1 are plotted against divergence angle and *D/C*. **(b)** Pairs with *J*=1 and *J*=2 are plotted for comparison. For reference purposes, point size is varied in order of occurrence in nature. The normal type with Fibonacci pairs (137.5°, solid lines in (a) and (b)) is outstandingly dominant, followed by major anomalies with 99.5° and 69° divergence angles (dashed line in (a) and (b)) and then by minor anomalies (78° and 151°, dotted lines in A). **(c)** *q:q'*=3:5. **(d)** 5:8. **(e)** 8:13. **(f)** 8:11. Spiral patterns (c-e) with an angle of 137.5° are observed on a shoot tip, while a similar pattern (f) does not occur.

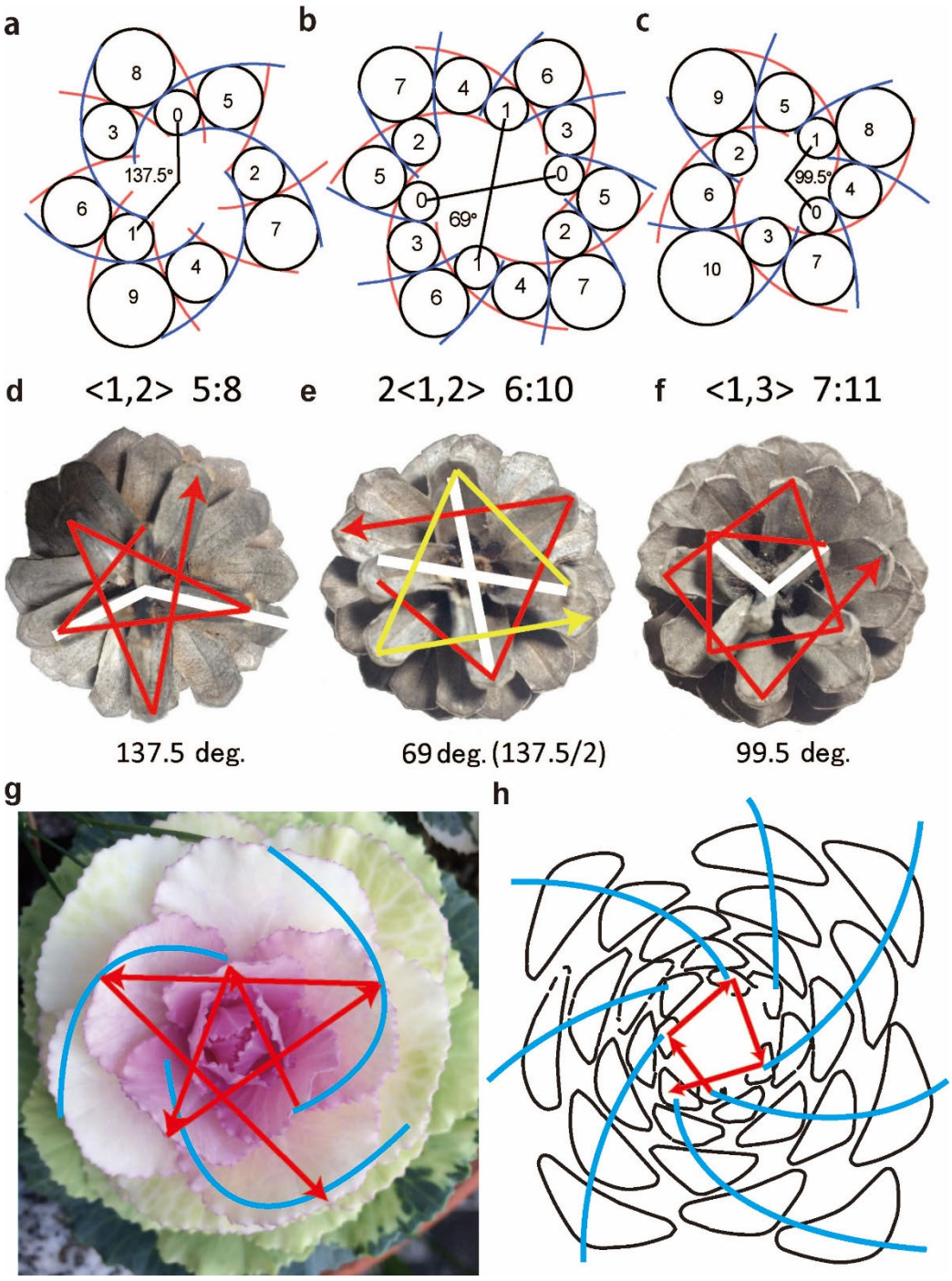

Figure 3. Normal and anomalous phyllotaxis types. **(a)** Normal 5:8 pattern (137.5°, *D/C*=0.106). **(b)** Anomalous 6:10 pattern (69°, *D/C*=0.085). **(c)** Anomalous 4:7 pattern (99.5°, *D/C*=0.124). **(d)** Normal 5:8 pattern. **(e)** Anomalous 6:10 pattern. **(f)** Anomalous

7:11 pattern. (d-f, *Pinus thunbergii*). **(g)** A normal 3:5 pattern of ornamental kale (*Brassica oleracea*). **(h)** An anomalous 4:7 pattern of daikon radish leaves (*Raphanus sativus*); redrawn and adapted (Koriba 1951).

Table 1: Cones from a *Pinus nigra* tree (Fierz 2015)

Type	*q:q'*	Number	$p \pm \sigma$
$\langle 1,2 \rangle$	8:13	**5838**	**0.970±0.002**
$2\langle 1,2 \rangle$	10:16	**69**	**0.012±0.001**
$\langle 1,3 \rangle$	7:11	**20**	**0.0033±0.0007**
$3\langle 1,2 \rangle$	9:15	**9**	**0.0015±0.0005**
$\langle 1,4 \rangle$	9:14	3	0.0005±0.0003
$\langle 2,5 \rangle$	7:12	3	0.0005±0.0003
$4\langle 1,2 \rangle$	8:12	**5**	**0.0008±0.0004**
$\langle 1,5 \rangle$	6:11	1	0.0002±0.0002
$\langle 4,9 \rangle$	9:13	2	0.0003±0.0002
$\langle 3,7 \rangle$	7:10	1	0.0002±0.0002
	Irregular	**49**	**0.008±0.001**
Total		6000	

Table 2: Normal and anomalous types in various conifers (Brousseau 1969)

	$\langle 1,2 \rangle$	Not $\langle 1,2 \rangle$	$p \pm \sigma$
Pinus contorta var. *murrayana*	884	8	**0.009±0.003**
Pinus jeffreyi	384	18	**0.05±0.01**
Pinus monticola	444	5	**0.011±0.005**
Pinus ponderosa	427	2	0.005±0.003
Pinus monophylla	400	5	**0.012±0.006**
Pinus balfouriana	424	36	**0.08±0.01**
Pinus attenuata	425	0	
Pinus radiata	354	7	**0.019±0.007**
Pinus muricata	193	0	
Pinus contorta	274	0	
Pseudotsuga menziesii	357	1	0.003±0.003

Two-step mechanism of spiral phyllotaxis

Authors: Takuya Okabe and Jin Yoshimura

Supplementary Materials

Supplementary Text

Lattice on a cylindrical surface

The position on a cylindrical surface is specified by the cylindrical coordinates (x, z), where x is measured around the girth $(-1/2 < x < 1/2)$ and z is parallel to the cylinder axis. For the moment, we assume that the girth of a cylinder is a unit of length, $C = 1$. Let P_0 be the 0th point at $(0,0)$. The next point P_1 is at (α, h), where α and h are the divergence angle and rise, respectively. The coordinates of the n-th point P_n $(n = 0,1,2,\cdots)$ are $(x_n, z_n) = (n\alpha - [n\alpha], nh)$. In the coordinate x_n, the nearest integer of number $n\alpha$, $[n\alpha]$, is subtracted to obtain $-1/2 < x_n < 1/2$. On a cylindrical surface, all the coordinates $(x, z) = (n, 0)$ $(n = 0,1,2,3,\cdots)$ are the same point, the origin (P_0) of the coordinate system.

A q spiral (parastichy) runs in the direction of $\overrightarrow{P_0P_q} = (x_q, y_q) = (q\alpha - p, qh)$, where p is the integer nearest to $q\alpha$. Similarly, the direction of a q' spiral is $\overrightarrow{P_0P_{q'}} = (q'\alpha - p', q'h)$, where p' is the integer nearest to $q'\alpha$. The four points $P_0P_qP_{q+q'}P_{q'}$ make a square of area $|\, pq' - p'q \,|\, h$. For the moment, let us assume that q and q' have no common divisor $(J = 1)$. Then, the lattice has a single point per rise, and the area of a unit cell should equal h. Therefore,

$$pq' - p'q = \pm 1.$$

This linear Diophantine equation has a unique solution (a positive integer pair) p and p' for given values of q and q'. For instance, $p = 2$ and $p' = 3$ for $q = 5$ and $q' = 8$. The mesh size of this $q{:}\,q'$ parastichy system is given by

$$D = OP_q = OP_{q'},$$

or

$$D^2 = (q\alpha - p)^2 + (qh)^2 = (q'\alpha - p')^2 + (q'h)^2.$$

The condition under which $\overrightarrow{OP_q}$ and $\overrightarrow{OP_{q'}}$ cross orthogonally is

$$\overrightarrow{OP_q} \cdot \overrightarrow{OP_{q'}} = (q\alpha - p)(q'\alpha - p') + qq'h^2 = 0.$$

As the solution for these equations, we obtain the following result:

$$\alpha = \frac{pq + p'q'}{q^2 + q'^2},$$

$$h = \frac{1}{q^2 + q'^2},$$

and

$$D^2 = \frac{1}{q^2 + q'^2}.$$

If the girth length C is retrieved, D and rise h are replaced with D/C and $h/C = (D/C)^2$, respectively. Note that h/C is called rise in the main text. In degrees, the divergence angle is 360α (Fig. 1(a,b)). The above result for α is the mathematical relation between the parastichy pair (q, q') and the divergence angle, which indicates that asking why some specific divergence angles (e.g., the golden angle) occur is equivalent to asking why some specific parastichy pairs occur. This is a biological problem of the living organism, which is outside

the scope of the present study.

If q and q' have a common divisor $J > 1$, one may use q/J and q'/J instead of q and q' in the discussion above. To avoid confusion, however, it is convenient to let q and q' have no common divisor except 1 ($J = 1$) and consider a $Jq{:}Jq'$ system for an arbitrary value of J ($= 1,2,3,\cdots$). Then, C, D, α and h are replaced by JC, D, α/J and h, respectively.

Organ size ratio

It is straightforward to geometrically explain the abovementioned result $D/C = 1/\sqrt{q^2 + q'^2}$, which is the square root of h/J. In effect, this is the Pythagorean theorem (see the main text and Fig. 1(b) for a simple way of making the lattice). In Supplementary Figure S1, a tilted square contains $q^2 + q'^2$ mesh points. As counted from a reference point $O = P_0$, the number n of the grid point $P = P_n$ lying directly above O is $q^2 + q'^2$ (i.e., $P = P_{q^2+q'^2}$). Hence, $OP = h(q^2 + q'^2)$ is equal to the girth $C = 1$.

The practical utility of the ratio D/C is manifested by transforming the square grid on a cylindrical surface (Fig. 1(g)) into a lattice of logarithmic spirals (Fig. 1(h)). Mathematically, the former's cylindrical coordinates (ρ, θ, z) and the latter's polar coordinates (r, θ) are related by the equation $z/\rho = \log r$. Since this transformation preserves the angle between crossing spirals, a square lattice on a cylindrical surface is mapped to a system of orthogonally intersecting logarithmic spirals on a plane. The transformed pattern is directly compared with the phyllotaxis pattern in a transverse cross-section of a shoot tip (bud) (Fig. 1(h), Fig. 2(c-h), Fig. 3(a-c)).

Supplementary Figure S1

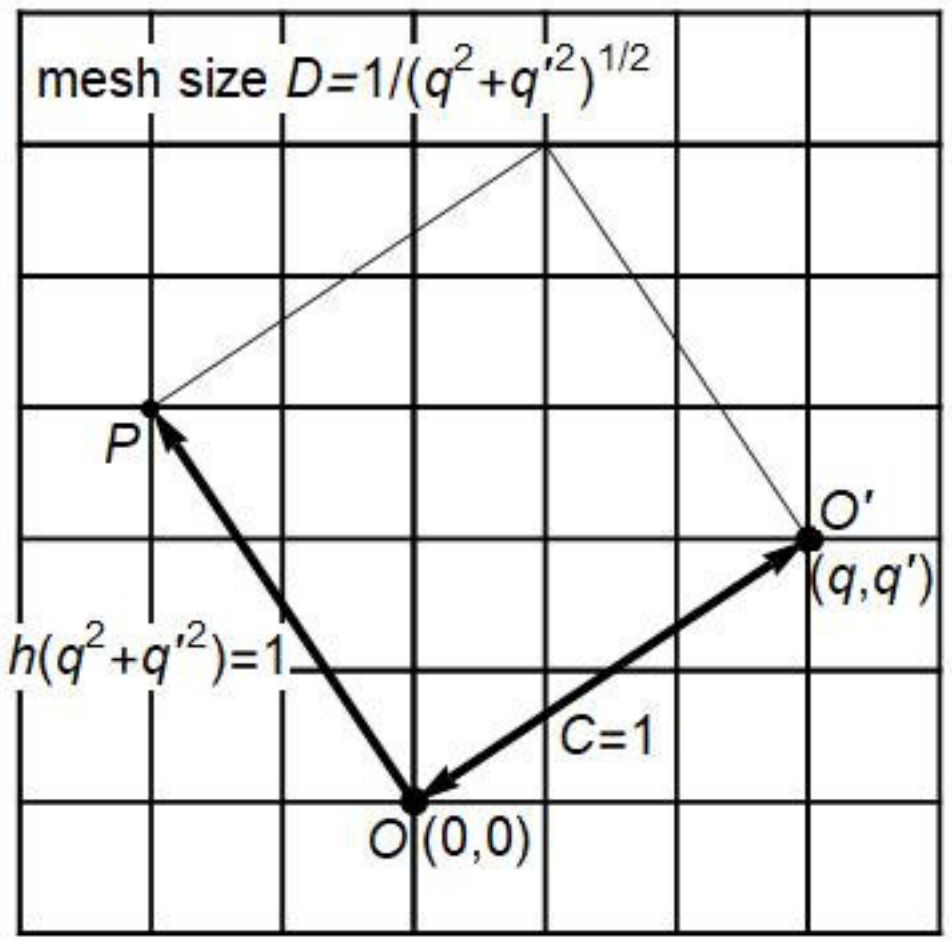

Supplementary Figure S1. Phyllotaxis grid pattern.